NeuroImage: Clinical 35 (2022) 103092

Contents lists available at ScienceDirect

NeuroImage: Clinical

journal homepage: www.elsevier.com/locate/ynicl

Effects of acute high intraocular pressure on red-green and blue-yellow cortical color responses in non-human primates

Mengwei Li [a,1], Xiaoxiao Chen [a,1], Nini Yuan [a,b,*], Yiliang Lu [b], Ye Liu [b], Hongliang Gong [b], Liling Qian [b], Ian Max Andolina [b], Jihong Wu [a,d,e], Shenghai Zhang [a,d,e], Niall McLoughlin [f], Xinghuai Sun [a,c,d,e,*], Wei Wang [b,g,*]

[a] Eye Institute and Department of Ophthalmology, Eye & ENT Hospital, Fudan University, Shanghai, China
[b] Institute of Neuroscience, Key Laboratory of Primate Neurobiology, Chinese Academy of Sciences Center for Excellence in Brain Science and Intelligence Technology, State Key Laboratory of Neuroscience, Chinese Academy of Sciences, Shanghai Center for Brain Science and Brain-Inspired Intelligence Technology, Shanghai, China
[c] State Key Laboratory of Medical Neurobiology and MOE Frontiers Center for Brain Science, Institutes of Brain Science, Fudan University, Shanghai, China
[d] NHC Key Laboratory of Myopia (Fudan University), Key Laboratory of Myopia, Chinese Academy of Medical Sciences, Shanghai, China
[e] Shanghai Key Laboratory of Visual Impairment and Restoration, Shanghai, China
[f] School of Optometry and Vision Science, University of Bradford, UK
[g] University of Chinese Academy of Sciences, Beijing, China

ARTICLE INFO

Keywords:
Glaucoma
Acute intraocular pressure elevation
Cortical color responses
Optical imaging
Macaque monkeys

ABSTRACT

Glaucoma is a leading cause of irreversible blindness worldwide, and intraocular pressure (IOP) is an established and modifiable risk factor for both chronic and acute glaucoma. The relationship between color vision deficits and chronic glaucoma has been described previously. However, the effects of acute glaucoma or acute primary angle closure, which has high prevalence in China, on color vision remains unclear. To address the above question, red-green or blue-yellow color responses in V1, V2, and V4 of seven rhesus macaques were monitored using intrinsic-signal optical imaging while monocular anterior chamber perfusions were performed to reversibly elevate IOP acutely over a clinically observed range of 30 to 90 mmHg. We found that the cortical population responses to both red-green and blue-yellow grating stimuli, systematically decreased as IOP increased from 30 to 90 mmHg. Although a similar decrement in magnitude was noted in V1, V2, and V4, blue-yellow responses were consistently more impaired than red-green responses at all levels of acute IOP elevation and in all monitored visual areas. This physiological study in non-human primates demonstrates that acute IOP elevations substantially depress the ability of the visual cortex to register color information. This effect is more severe for blue-yellow responses than for red-green responses, suggesting selective impairment of the koniocellular pathways compared with the parvocellular pathways. Together, we infer that blue-yellow color vision might be the most vulnerable visual function in acute glaucoma patients.

1. Introduction

Glaucoma, the leading cause of blindness worldwide, is a group of diseases characterized by progressive retinal ganglion cell (RGC) death (Jonas et al., 2017; Weinreb et al., 2014). Elevated intraocular pressure (IOP) is one of major risk factors for the development and progression of glaucoma (Sun et al., 2017; Weinreb et al., 2016). The two main forms of glaucoma are classified by either an acute or chronic rise in IOP. The damage caused by high IOP starts with RGCs in the retina, but ultimately affects human visual function, of which color vision is one of the central

* Corresponding authors at: Institute of Neuroscience, Key Laboratory of Primate Neurobiology, Chinese Academy of Sciences Center for Excellence in Brain Science and Intelligence Technology, State Key Laboratory of Neuroscience, Chinese Academy of Sciences, Shanghai Center for Brain Science and Brain-Inspired Intelligence Technology, 320 Yueyang Road, Shanghai 200031, China (N. Yuan); Eye Institute and Department of Ophthalmology, Eye & ENT Hospital, Fudan University, 83 Fenyang Road, Shanghai 200031, China (X. Sun); Institute of Neuroscience, Key Laboratory of Primate Neurobiology, Chinese Academy of Sciences Center for Excellence in Brain Science and Intelligence Technology, State Key Laboratory of Neuroscience, Chinese Academy of Sciences, Shanghai Center for Brain Science and Brain-Inspired Intelligence Technology, 320 Yueyang Road, Shanghai 200031, China (W. Wang).
E-mail addresses: nnyuan@ion.ac.cn (N. Yuan), xhsun@shmu.edu.cn (X. Sun), w.wang@ion.ac.cn (W. Wang).
[1] These authors contributed equally to the work.

https://doi.org/10.1016/j.nicl.2022.103092
Received 26 March 2022; Received in revised form 17 May 2022; Accepted 18 June 2022
Available online 21 June 2022

components. For chronic glaucoma patients, acquired color vision deficiencies are common and these color perception impairments can even be a precursor to visual field loss (Bayer et al., 2020; Drance et al., 1981; Greenstein et al., 1996; Nork, 2000; Pacheco-Cutillas et al., 1999; Pearson et al., 2001). Meanwhile, it has been reported that the color vision anomaly seen with elevated IOP is a vital sign for the conversion from ocular hypertension to glaucoma (Papaconstantinou et al., 2009; Poinoosawmy et al., 1980; Sample et al., 1986). Furthermore, most previous research suggests that glaucoma-related color vison defects mainly occur in the blue-yellow spectrum rather than in the red-green spectrum (Gunduz et al., 1988; Nuzzi et al., 1997; Pacheco-Cutillas et al., 1999; Poinoosawmy et al., 1980; Sample et al., 1988; Sample et al., 1986). Based on these findings, blue-on-yellow perimetry has been designed and shown to be more effective in predicting early glaucomatous visual field defects when compared to conventional white-on-white perimetry (Polo et al., 2002; Racette and Sample, 2003; Sample, 2000). These studies have concentrated on chronic glaucoma or ocular hypertension, in which the IOP gradually increases and patients are usually asymptomatic. However, acute glaucoma or acute primary angle closure, which has higher prevalence in China (Foster and Johnson, 2001; Song et al., 2017), can cause sharp IOP elevation with obvious symptoms (sudden headache, blurred vision, eye pain and redness, etc.). The effect of acute high IOP on human color vision remains unclear. Moreover, the established relationship between color vision deficits and glaucoma are mainly based on psychophysical experiments, and to date, there have been very limited studies with direct objective physiological detection of color responses (Dussan Molinos et al., 2021; Korth et al., 1994). Therefore, the immediate physiological effects of acute high IOP on color vision has yet to be investigated.

Color vision starts with the absorption of visible light by three types of cone photoreceptors, termed long-wavelength (L or "red"), medium-wavelength (M or "green"), and short-wavelength (S or "blue") sensitive cones in the retina. Then the cone signals are transformed into two forms of color-opponent signals: L versus M ("red" versus "green"), and S versus L + M ("blue" versus "yellow"), that are transmitted from midget ganglion cells and small-field bistratified ganglion cells through the parvocellular and koniocellular layers of the lateral geniculate nucleus (LGN), thus forming parvocellular and koniocellular color pathways that enter the visual cortex for further processing (Conway, 2014; Conway et al., 2010; Hendry and Reid, 2000; Liu et al., 2020; Martin, 1998). The cytochrome oxidase (CO) blobs of the primary visual cortex (V1) are the first cortical site of parvocellular and koniocellular convergence, with the suggestion that cell classes of CO blobs are sensitive to either red-green or blue-yellow color contrast (Gegenfurtner, 2003; Hubel and Livingstone, 1987; Landisman and Ts'O, 2002; Lu and Roe, 2008). These color signals are then relayed from the CO blobs of V1 through the CO thin stripes of the secondary visual cortex (V2) to color-specialized domains of V4 referred to as "globs" (Fig. 1**A**) (Conway et al., 2007; Lu and Roe, 2008; Tanigawa et al., 2010). Therefore, color deficits in differentiating cortical responses to red-green and blue-yellow color contrast could indicate the extent of impairment of parvocellular and koniocellular color pathways.

To address the above clinical question, we sharply elevated IOP in macaque monkeys using anterior chamber perfusion to examine the immediate effect of acute high IOP on color responses. We measured cortical population responses to red-green or blue-yellow color contrast across V1, V2, and V4 by taking advantage of the high spatial resolution of intrinsic-signal optical imaging, comparing the differences between red-green and blue-yellow color responses under acute high IOP (Fig. 1**B**). In the present study, we found that acute IOP elevations depressed color vision, and blue-yellow responses were more impaired than red-green responses across V1, V2 and V4 during acute IOP

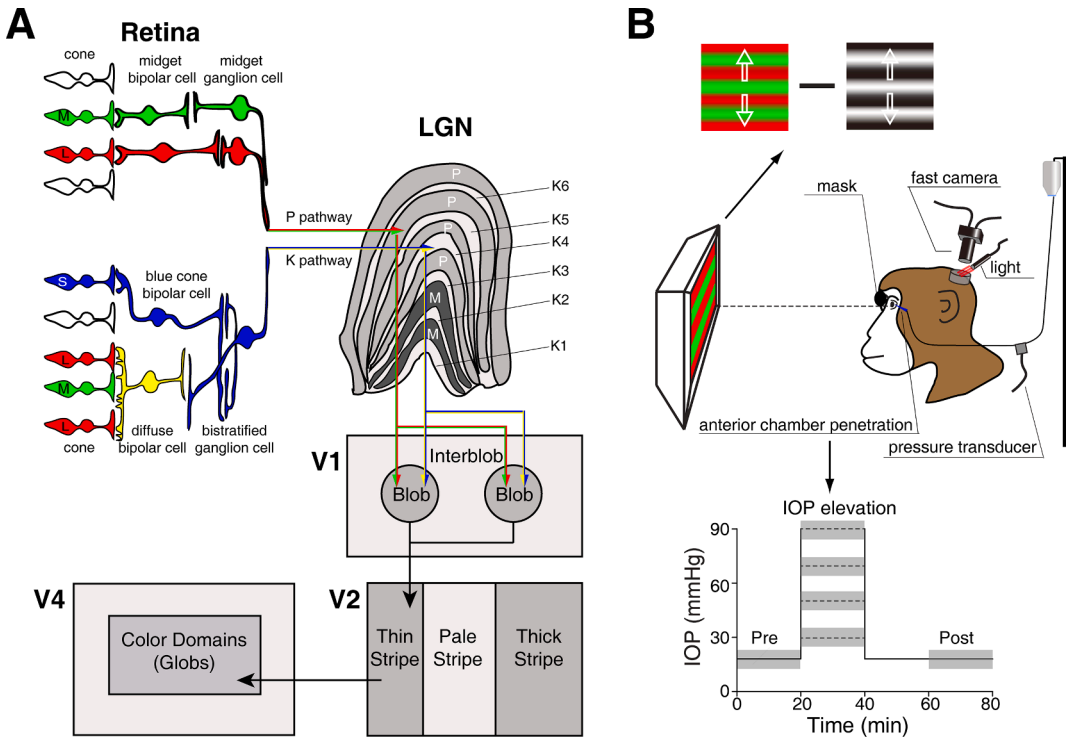

Fig. 1. Schematics of chromatic processing in the visual pathways and the experimental paradigm. (A) Anatomical modular substructure of color parallel pathways from retina to V1-V2-V4 cortex. In the retina, after the trichromatic sampling of the spectrum by long-, medium-, and short-wavelength (L, M, and S) sensitive cones, color signal is transmitted by two pairs of color-opponency: red-green and blue-yellow, thus forming P and K color pathways entering the P and K layers of the LGN. These two color streams converge at the blobs of V1 and then relay information to the thin stripes of V2 and to the color domains ("globs") of V4 for further processing. P: parvocellular; K: koniocellular; M: magnocellular. (B) Experimental setup. Acute and stepwise IOP elevations (30, 50, 70, and 90 mmHg) were conducted reversibly by anterior chamber perfusion with irrigating solution, while population activities to color stimuli in visual areas V1, V2, and V4 were recorded by our optical imaging system. (For interpretation of the references to color in this figure legend, the reader is referred to the web version of this article.)

elevation, indicating selective impairment of the koniocellular pathway compared with the parvocellular pathway. Our results provide suggestive evidence of the immediate effect of acute high IOP on cortical color vision in glaucoma patients.

2. Materials and methods

2.1. Animal preparation and maintenance

The subjects in this acute experiment were seven adult rhesus macaques (*Macaca mulatta*, four males and three females, 4–12 years old, weighing 5.9–10.2 kg). These macaques were the same animals used in a previous report (Li et al., 2019), that examined the impact of acute IOP elevation on the visual acuity. All surgical and experimental procedures were approved by the Animal Ethics Committee of the Eye and ENT Hospital of Fudan University (Shanghai, China), and were conducted in accordance with ARVO Statement for the Use of Animals in Ophthalmic and Vision Research. Access to data by qualified investigators (i.e., affiliated with accredited academic and research institutions) are subject to scientific and ethical review. Completion of a material transfer agreement signed by an institutional official will be required in order to access the data.

The animals were prepared and maintained for simultaneous optical imaging of intrinsic-signals in V1, V2, and V4 as previously described (An et al., 2012; Li et al., 2019; Liu et al., 2020; Lu et al., 2018; Yuan et al., 2020). Anesthesia was first induced with ketamine hydrochloride (15 mg/kg, i.m.) for tracheal and venous cannulation, followed by gaseous anesthesia (isoflurane 1–2% in 2:1 N_2O:O_2) during subsequent surgical operations. Craniotomies were performed to expose V1 and V2 on one side of the skull and V1, V2, and V4 on the other side of the skull in six monkeys, while V1 and V2 was exposed on both sides of the skull in another monkey. The lunate sulcus (LS) and superior temporal sulcus (STS) were used as cortical landmarks to obtain V1, V2, and V4 (V1 & V2: areas posterior to LS; V4: areas between LS and STS). A 30 mm stainless steel chamber was secured on the skull with dental cement, filled with warm silicon oil (DMPS-5X; Sigma-Aldrich Corp., St. Louis, MO, USA) and sealed with a coverslip after a durotomy. Subsequent anesthesia and paralysis for intrinsic-signal optical imaging were established with propofol (4–5 mg/kg/h, i.v.) and vecuronium bromide (0.16 mg/kg/h, i.v.), respectively. Supplemental fluids (sodium lactate Ringer's solution and 5% glucose, i.v.) were maintained and adjusted according to urinary output. Tropicamide-phenylephrine ophthalmic solution (Santen Pharmaceutical Cor., Ltd. Japan) was applied periodically to dilate pupils. Contact lenses were fitted to protect the corneas and the base curves of contact lenses were selected using a slit ophthalmoscope to ensure the eyes were focused on the stimulus plane. Electrocardiography, temperature, respiratory rate, oxygen saturation, and expired CO_2 were continuously monitored throughout the experiment and the anesthesia depth was confirmed by reflex tests. Each monkey was recorded for 5–6 days and was euthanized by an overdose of sodium pentobarbital (~200 mg/kg) at the end of the experiment.

2.2. Acute elevation of IOP

To manipulate the IOP in an eye, a 27-gauge needle connected with a cannula was inserted into the anterior chamber through the corneoscleral limbus. The cannula led to a three-way switch, and then to a pressure transducer with a height-adjustable reservoir containing ionic-balanced intraocular irrigating solution (SINQI Pharmaceutical Cor., China) for IOP manipulation (Fig. 1**B**). Normal IOP was set at approximately 15–18 mmHg according to the IOP readout immediately after anterior chamber penetration. Four levels of IOP elevation (30, 50, 70, and 90 mmHg) were used in a stepwise manner to evaluate the effect of high IOP on the cortical responses to the red-green or blue-yellow color stimuli. Our previous research in cats and monkeys has demonstrated that after transient (20 min) IOP elevation, cortical responses gradually return to the level before IOP elevation (Li et al., 2019; Yuan et al., 2020). Therefore, the duration of IOP elevation each time in the experiment lasted for a short period of approximately 18–20 min, with recovery periods of 20 min interleaved (Fig. 1**B**). Throughout the experiment, the manipulated eye was routinely examined by ophthalmoscope. During the transient IOP elevation, no corneal edema, cataract, or refractive errors were observed in our experimental setup in the manipulated eyes.

2.3. Visual stimuli

Visual stimuli were presented on a gamma-corrected CRT monitor (1280x960 pixels, 100 Hz, Sony G520, 21 in., Tokyo, Japan) covering 40° x 30° visual angle, placed 57 cm in front of the animal's eyes. The monitor was calibrated by SpectroCAL MKII Spectroradiometer (Cambridge Research Systems). The fovea and other retinal landmarks of the manipulated eye were back projected to the screen center using a reversing ophthalmoscope. Full-screen visual stimuli were generated with PSYCHTOOLBOX-3 (https://psychtoolbox.org) running in MATLAB 2015b (MathWorks, Natick, MA, USA). To identify the V1/V2 border using the ocular dominance test, we presented the same sinusoidal gratings monocularly, to each eye in turn (Li et al., 2019; Lu et al., 2018). In all IOP elevation experiments, visual stimuli were displayed monocularly (to the manipulated eye) and the other eye was occluded. For mapping color preference domains, we used isoluminant red-green and blue-yellow square-wave gratings, each chromatic grating being contrasted with an achromatic black-white grating of the same low spatial frequency (0.5 cycle/degree), the same temporal frequency (2 Hz) and the same orientation (0°) (Liu et al., 2020).

2.4. Optical imaging of Intrinsic-signal and analysis

Optical imaging system used in our experiment has been described in detail previously (An et al., 2012; Li et al., 2019; Liu et al., 2020; Lu et al., 2018; Yuan et al., 2020). Briefly, two Dalsa Pantera 1 M60 CCD cameras (Waterloo, Ontario, Canada) combined with two telecentric 55 mm f2.8 video lenses (Tokyo, Japan) were applied to simultaneously record images of reflectance change corresponding to cortical population responses from regions of interest (ROI) in visual areas in two chambers, one on each side of the skull. 550 ± 10 nm (green) illumination was used for mapping blood vessels, and 630 ± 10 nm (red) illumination for optical imaging of intrinsic optical signals associated with neural activity. For each trial, two conditions including a pair of contrasting visual stimuli were sequentially displayed. For example, chromatic versus achromatic gratings (e.g., red/green-black/white) were used to activate color maps. Visual responses for each condition were recorded for a period of 8 s, including 1 s before stimulus onset. The interstimulus interval was 13 s. During each phase of optical imaging (before, during or 20 min after IOP elevation), 32 trials were repeatedly collected, taking approximately 18–20 min. Following IOP elevation, IOP was restored to normal and no testing was performed for 20 min, thus allowing for ganglion cell recovery from the effect of transient IOP elevation.

To achieve cortical population responses, a single-condition map was first constructed and the value of each pixel in the single-condition map represents the percent change of the illumination reflectance (ΔR/R), calculated as $(R_{avg} - R_0)/R_0$, in which R_0 represents a blank frame (the average response for the 1 s before stimulus onset), and R_{avg} is the average responses a period of 2–6 s after stimulus onset. A differential color map was then created by pixelwise subtraction of two single-condition maps activated by a stimulus pair (chromatic versus achromatic gratings such as red/green-black/white and blue/yellow-black/white) (An et al., 2012; Liu et al., 2020). To reduce the noise associated with blood vessels and other noisy regions, a gray mask was generated based on a cross-trial variability calculation and modified empirically by hand (Li et al., 2019; Yuan et al., 2020). Pixels within the

mask were then excluded in subsequent quantitative analysis. For visualization, the images were high-pass filtered (1.1–1.2 mm in diameter) and smoothed (106–306 μm in diameter) by circular averaging filters to suppress low- and high-frequency noise while avoiding signal distortion. For the quantification of the color response amplitude, responsive patches in a differential map were defined as pixels being 1.5 SDs above baseline, and the value of ΔR/R in the responsive patches preferring the first stimulus condition (chromatic gratings) of a trial was treated as the measure of response amplitude. We took the cortical population response amplitude before IOP elevation as the control, and then calculated the response ratio (IOP/control, %) during IOP elevation as an index to evaluate the IOP effects. The boundary of V1 and V2 was determined using the ocular dominance mapping method, which produced stripe-like compartments perpendicular to the border between V1 and V2, as described earlier (Ts'O et al., 1990).

2.5. Statistical analysis

SPSS (version 22.0 for windows, SPSS Inc., Chicago, IL, USA) was used for statistical comparison of cortical responses across 14 hemispheres in seven monkeys. Due to the exposure of V1 and V2 on one side of the skull and V1, V2, and V4 on the other side of the skull in six monkeys, while V1 and V2 on both sides of the skull in one monkey, measurements from 14 V1, 14 V2, and six V4 regions were included in the final analysis. All data are shown graphically as mean ± standard error of the mean (SEM). Paired t tests were performed to compare the cortical color response amplitudes between control and each IOP elevation condition, and the cortical response ratios between red-green and blue-yellow color stimuli in the same IOP elevation. One-way ANOVA was used for the comparison of the cortical response ratios among V1, V2, and V4 in the same IOP. The significance level was set at 0.05 (two-tailed).

3. Results

3.1. Higher acute IOP elevations generate progressively greater decrements in color responses

To examine the impact of different IOP levels on the cortical responses to color stimuli, a range of IOP elevations (30, 50, 70, and 90 mmHg) were successively applied to seven monkeys. An example hemisphere with V1 and V2 exposed shows that the monocular cortical color responses to both red-green and blue yellow stimuli progressively decreased as IOP elevated, without any change in the location of the color-specialized domains (black patches) (Fig. 2). This trend is also demonstrated in another example hemisphere with V1, V2 and V4 exposed (Fig. 3). The cortical color responses were calculated as the pixel intensity of the black patches. Averaging across 14 hemispheres (including 14 V1, 14 V2, and six V4 regions) in seven monkeys, almost all IOP elevations from 30 to 90 mmHg significantly depressed cortical color responses in V1, V2 and V4 when compared with their controls. This was true for red-green responses (Fig. 4**A and** Table 1) and for blue-yellow responses (Fig. 4**B and** Table 2). Note that although the red-green responses in V4 when the IOP was elevated 30 mmHg was not significantly different from the control responses, there was still a clear trend of a decline in response magnitude. In addition, we found that the elevation of each IOP level had a similar decline of cortical color responses among V1, V2, and V4 (all $P > 0.05$, one-way ANOVA; Fig. 4**C**).

3.2. Acute high IOP affects blue-yellow responses more adversely than red-green responses

Red-green and blue-yellow are two forms of color-opponent channels in color processing and are indicative of the state of the parvocellular and koniocellular pathways in the primate visual system. Therefore, we further compared the differential effect of acute IOP elevations on the

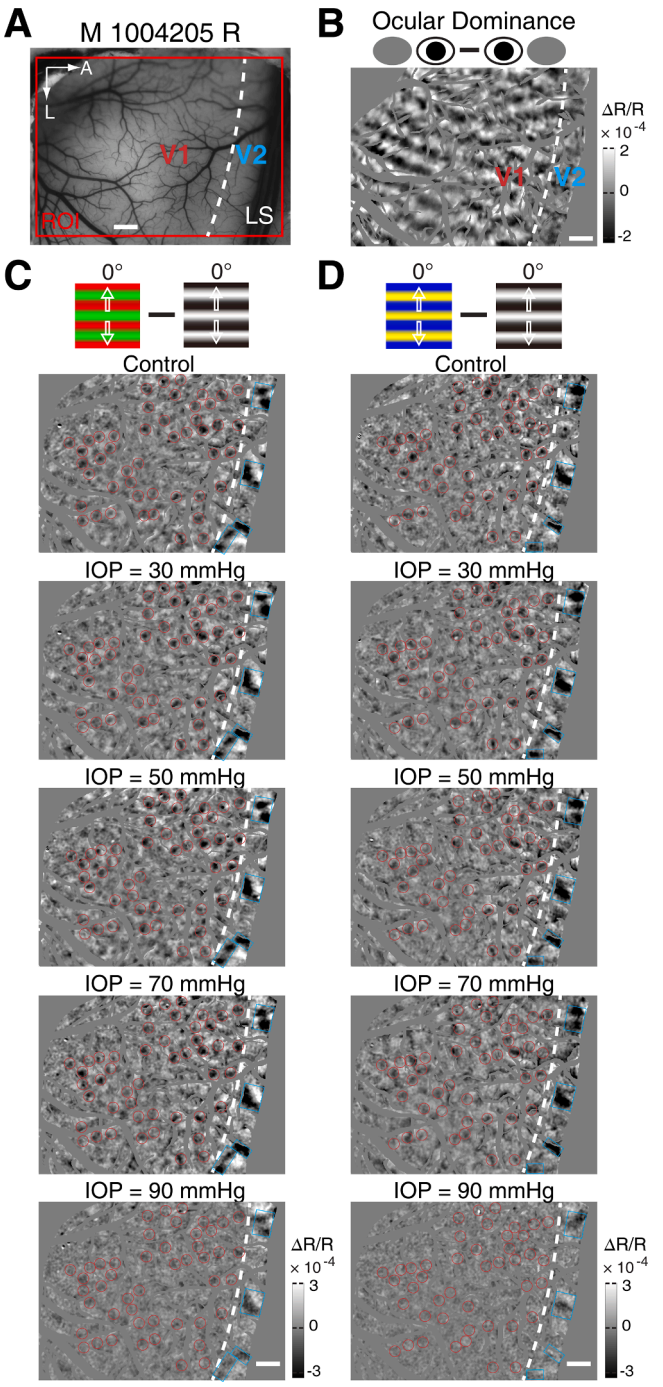

Fig. 2. Example red-green and blue-yellow color maps in V1 and V2 during different levels of acute IOP elevation. (A) The cortical surface exposed V1 and V2 in the right hemisphere of monkey M1004205 and the ROI (red box) used for optical imaging. LS, lunate sulcus; A, anterior; L, lateral. (B) Differential ocular dominance map. Note that stripe-like compartments run approximately perpendicular to the V1/V2 border (the white dotted line) and are absent in V2. (C) Comparison of color responses evoked by red-green stimuli across different levels of IOP elevations (30, 50, 70, and 90 mmHg) in V1 and V2. (D) Comparison of color responses evoked by blue-yellow stimuli across different levels of IOP elevations (30, 50, 70, and 90 mmHg) in V1 and V2. Note that the cortical responses before each IOP elevation were taken as controls and the controls shown in (C) and (D) are for IOP elevation for 30 mmHg. Color responsive sites (dark patches) in V1 and V2 (known as blobs and thin stripes) are indicated by red circles and calamine blue box respectively. Scale bar, 1 mm. (For interpretation of the references to color in this figure legend, the reader is referred to the web version of this article.)

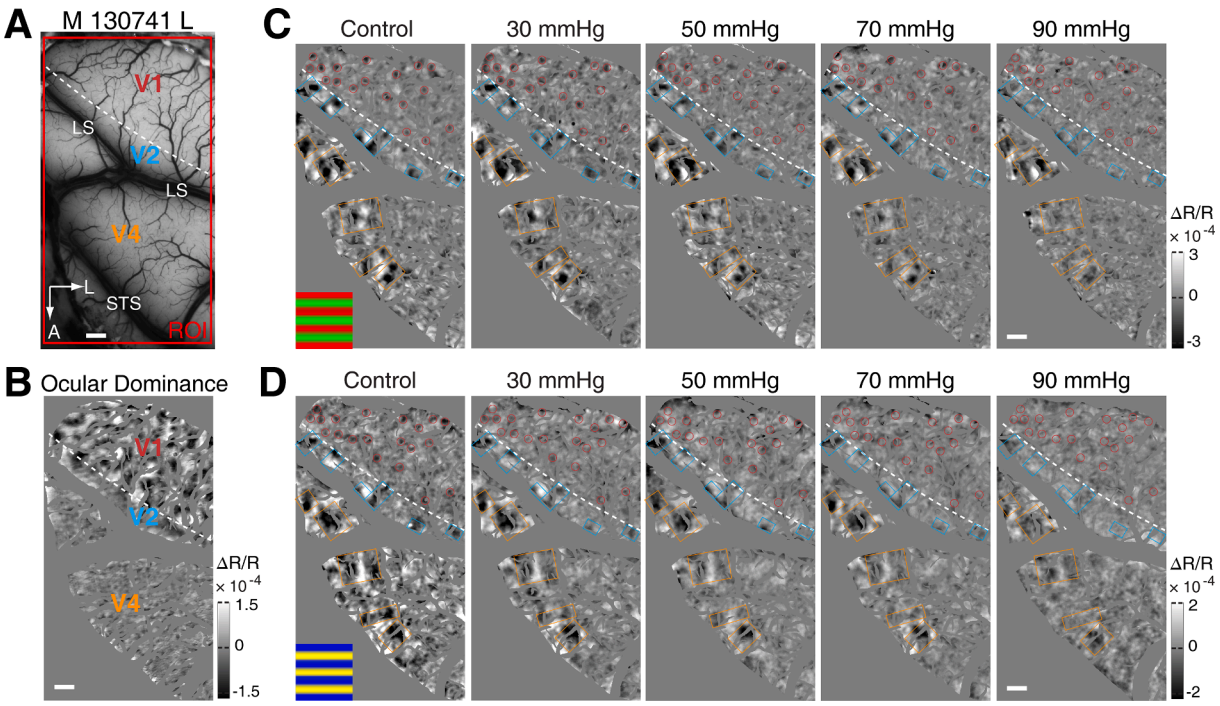

Fig. 3. Example red-green and blue-yellow color maps in V1, V2, and V4 during different levels of acute IOP elevation. (A) The cortical vascular pattern of simultaneously recorded V1, V2, and V4 in monkey (M130741) left hemisphere and the ROI (red box) used for optical imaging. LS, lunate sulcus; STS, superior temporal sulcus; A, anterior; L, lateral. (B) Ocular dominance map used for dividing the border of V1 and V2 (the white dotted line). (C) Comparison of color responses evoked by red-green stimuli across different levels of IOP elevations (30, 50, 70, and 90 mmHg) in V1, V2, and V4. (D) Comparison of color responses evoked by blue-yellow stimuli across different levels of IOP elevations (30, 50, 70, and 90 mmHg) in V1, V2, and V4. Note that the cortical responses before each IOP elevation were taken as controls and the controls shown in (C) and (D) are for IOP elevation for 30 mmHg. Color responsive domains in V1, V2, and V4 are shown by red circles, calamine blue box, and orange box respectively. Scale bar, 1 mm. (For interpretation of the references to color in this figure legend, the reader is referred to the web version of this article.)

red-green and blue-yellow cortical responses in the same preparation. Fig. 2**C, D** and Fig. 3**C, D** respectively present an example V1-V2 hemisphere and V1-V2-V4 hemisphere showing color maps elicited by red-green and blue-yellow contrast stimuli under different IOP levels. The blue-yellow responses seemed to become weaker when compared with the red-green responses during IOP elevation. We then calculated the average response magnitudes across all 14 hemispheres and found that the blue-yellow response ratios (with respect to control) were consistently smaller than red-green response ratios during all levels of acute IOP elevation across V1, V2, and V4 (Fig. 5 **and** Table 3). These results reveal that during acute IOP elevation, blue-yellow responses are more impaired than red-green responses across V1, V2 and V4, indicating that acute high IOP is relatively more deleterious for the koniocellular pathway compared to the parvocellular pathway.

4. Discussion

Form/shape, motion, and color are three main functions of human vision. The damaging impacts of acutely increased IOP on cortical form and motion responses have been revealed in both monkey and cat (Chen et al., 2003; Li et al., 2019; Yuan et al., 2020). However, the relationship between immediate acute high IOP and color vision is still unclear. In the present study, we found that acute IOP elevations depressed the ability of the visual cortex to register color information in multiple visual areas of the macaque monkey, an effect that was more pronounced for blue-yellow responses than for red-green responses. These results provide suggestive physiological evidence that acute high IOP may first impair blue-yellow color vision in primates.

4.1. *Immediate effect of elevated IOP on color processing*

Human and macaque color vision originates from the trichromatic sampling of the spectrum by three types of cone photoreceptors in the retina. Then the trichromatic signals are processed into two pairs of color-opponent channels: red-green and blue-yellow (Conway, 2014; Conway et al., 2010). At the level of RGC, which is the site injured by increased IOP (Jonas et al., 2017), the red-green color information is encoded by midget ganglion cells while blue-yellow color information is coded by small-field bistratified ganglion cells (Martin, 1998). These two types of RGCs carry separate color streams to the parvocellular and koniocellular layers of LGN, thus forming two parallel pathways (Conway, 2014; Conway et al., 2010; Gegenfurtner, 2003). The parvocellular and koniocellular pathways form the basis for all subsequent color processing in V1, V2, and V4 (see Fig. 1). Although the primary injured site resulting from high IOP is in the retina, it ultimately affects the whole visual pathway. Therefore, as expected, we found that the cortical color responses, both red-green and blue-yellow, decreased as the IOP increased. In addition, our results show that there exists a similar magnitude of response decrement within V1, V2, and V4, which is somewhat distinct from our recent cat study revealing that IOP elevation suppresses cortical responses more severely in area 17 (likely homologous to V1 in primates) than in area 18 (likely homologous to V2 in primates) (Yuan et al., 2020). We speculate that this is largely because the visual pathways between primates and felines are different: in primates, all parallel pathways enter V1 and then transmit through V1-V2-V4 in series (Nassi and Callaway, 2009), whereas primary and secondary visual areas of feline cortex receive separate parallel pathways directly (Ferster, 1992).

As is well known, elevated IOP is the most critical risk factor for glaucoma (Jonas et al., 2017). Acquired color vision defects associated

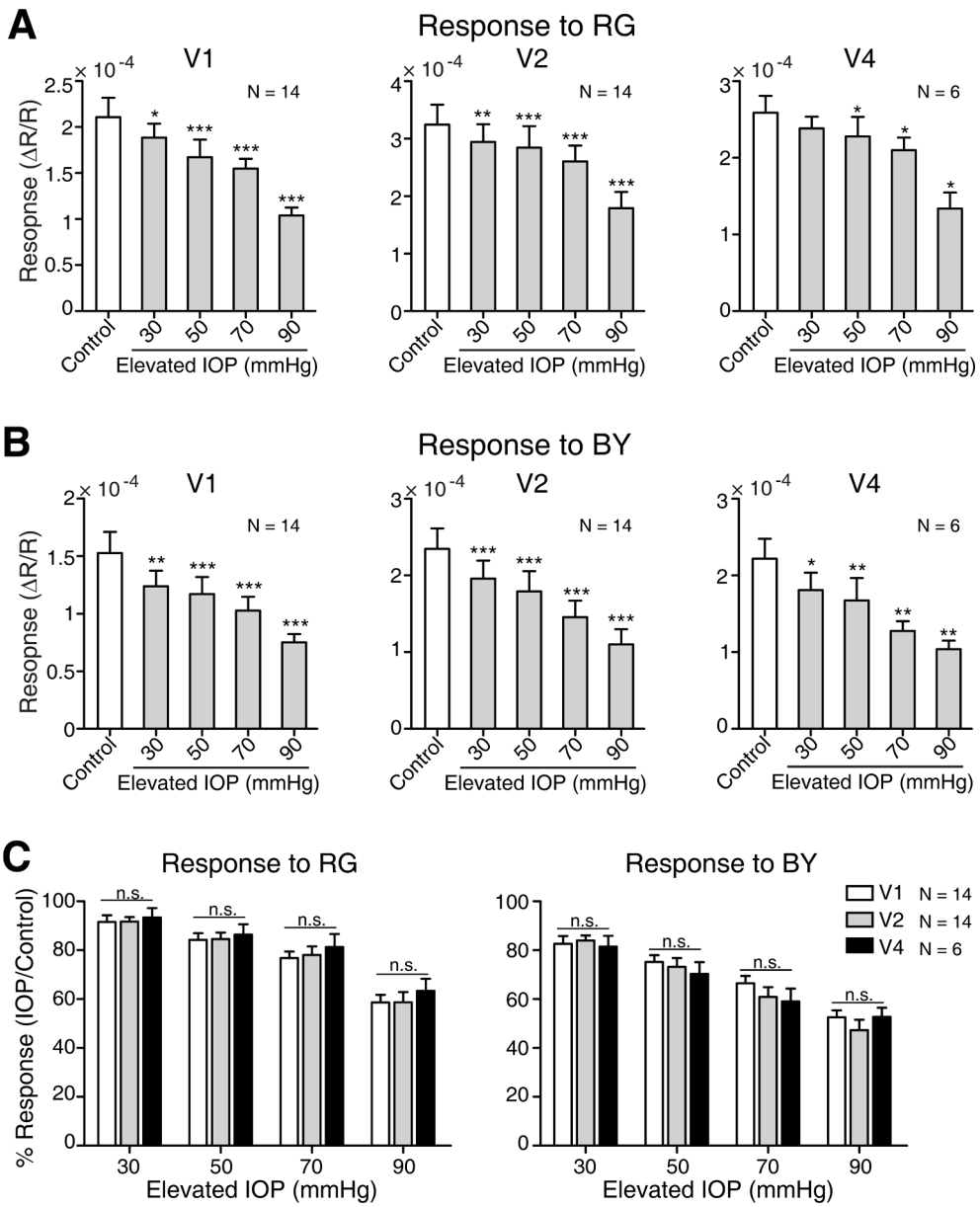

Fig. 4. Statistics of cortical color responses during acute IOP elevations in V1, V2, and V4 across animals. (A) Comparison of the average cortical responses to red-green (RG) stimuli during each IOP elevation with the control condition. (B) Comparison of the average cortical responses to blue-yellow (BY) stimuli during each IOP elevation with the control condition. Controls were taken as cortical responses before each acute IOP elevation. The control shown is for IOP elevation of 30 mmHg. There were no significant differences in response amplitude among the controls for each IOP condition (RG: V1: $F = 0.432$, $P = 0.731$; V2: $F = 0.228$, $P = 0.876$; V4: $F = 0.487$, $P = 0.695$; BY: V1: $F = 0.029$, $P = 0.993$; V2: $F = 0.043$, $P = 0.998$; V4: $F = 0.172$, $P = 0.914$; one-way ANOVA). $^{***}P < 0.001$, $^{**}P < 0.01$, $^{*}P < 0.05$. (C) Comparison of the color response ratio (IOP/control) among V1, V2 and V4 during each IOP elevation. n.s. represents $P > 0.05$. N, hemisphere numbers. Error bar denotes SEM.

Table 1
P values for comparison of average cortical responses to red-green stimuli during each IOP elevation with the control condition (paired-*t* test).

IOP	V1 (N = 14)	V2 (N = 14)	V4 (N = 6)
30 mmHg	0.018	1.3E-03	0.144
50 mmHg	6.2E-04	1.1E-04	0.038
70 mmHg	4.6E-05	3.8E-04	0.034
90 mmHg	8.0E-06	2.6E-05	0.011

N, hemisphere numbers.

Table 2
P values for comparison of average cortical responses to blue-yellow stimuli during each IOP elevation with the control condition (paired-*t* test).

IOP	V1 (N = 14)	V2 (N = 14)	V4 (N = 6)
30 mmHg	1.0E-03	1.4E-04	0.015
50 mmHg	8.0E-06	8.0E-06	0.002
70 mmHg	9.0E-06	1.0E-06	0.005
90 mmHg	7.0E-06	2.0E-06	0.003

N, hemisphere numbers.

with glaucoma have been described since the 19th century and controversy surrounded whether red-green defects or blue-yellow defects or a general loss of chromatic discrimination accompanied glaucomatous neuropathy in early studies (Alvarez et al., 1997; Austin, 1974; Drance et al., 1981; Kalmus et al., 1974; Pacheco-Cutillas et al., 1999). With the development of computer-generated color tests and the control of confounding factors such as lens density and pupil size, most psychophysical investigations indicate that blue-yellow defects predominate in glaucoma patients (Gunduz et al., 1988; Nuzzi et al., 1997; Poinoosawmy et al., 1980; Sample et al., 1986). Furthermore, it has been suggested that blue-on-yellow (short-wavelength) perimetry is more sensitive than standard white-on-white automated perimetry to measure glaucomatous loss (Polo et al., 2002; Racette and Sample, 2003; Sample, 2000). However, a blue-yellow abnormality has also been found in normal-tension glaucoma eyes (Yamagami et al., 1995). Therefore, it remains unclear whether increased IOP is the direct reason for color

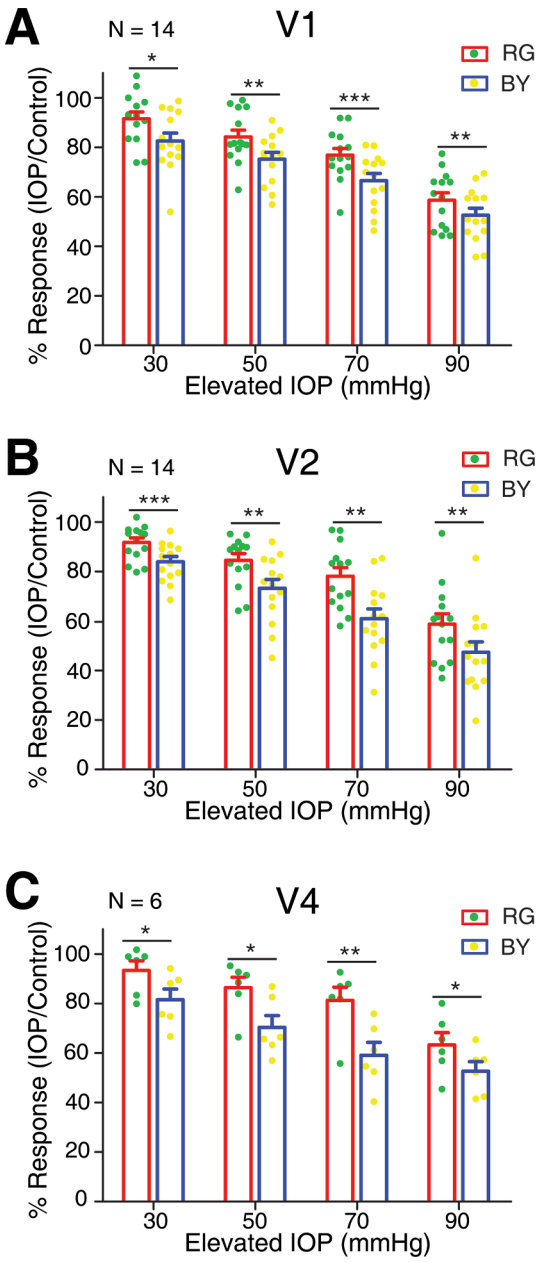

Fig. 5. Comparison of cortical color response ratio (IOP/control) between red-green (RG) and blue-yellow (BY) in V1 (A), V2 (B), and V4 (C) during each acute IOP elevation. ***$P < 0.001$, **$P < 0.01$, *$P < 0.05$. N, hemisphere numbers. Error bar denotes SEM. (For interpretation of the references to color in this figure legend, the reader is referred to the web version of this article.)

Table 3
P values for comparison of cortical color response ratio (IOP/control) between red-green and blue-yellow in V1, V2, and V4 during each IOP elevation (paired-*t* test).

IOP	V1 (N = 14)	V2 (N = 14)	V4 (N = 6)
30 mmHg	0.012	4.2E-04	0.012
50 mmHg	9.2E-03	1.7E-03	0.047
70 mmHg	5.0E-04	2.0E-03	4.6E-03
90 mmHg	3.8E-03	5.5E-03	0.027

N, hemisphere numbers.

vision defects in glaucoma eyes since glaucoma also involves non IOP-induced mechanisms (Yamagami et al., 1995). Our knowledge about color vision defects in glaucoma patients comes from numerous psychophysical studies. To date, the direct physiological assessment of the relationship between the immediate IOP effect and color responses has been lacking. The present study, however, sheds light on the immediate effect of high IOP on color processing by physiologically examining cortical population responses.

4.2. Comparison of acute and chronic IOP elevations on color vision

In the present study, an acute high-IOP monkey model was used and our transient acute IOP elevations did not cause irreversible damage to the RGCs. Similarly, clinical ocular hypertension is usually regarded as a form of chronic IOP elevation higher than the mean of a normal adult population but without glaucomatous optic disk damage (Lee and Wilson, 2003). Therefore, we can compare color vision defects in acute IOP elevation with those in chronic ocular hypertension. Many previous psychophysical studies suggest that the biggest defect in patients suffering from chronic ocular hypertension occurs within the blue-yellow spectrum rather than the red-green spectrum and that this blue-yellow color vision anomaly may indicate a sign for the conversion to glaucoma (Gunduz et al., 1988; Heron et al., 1988; Mantyjarvi and Terasvirta, 1992; Papaconstantinou et al., 2009; Poinoosawmy et al., 1980; Sample et al., 1986). Our present study demonstrates that acute IOP elevations depress blue-yellow responses more than red-green responses in multiple visual areas of macaque monkeys. Taken together, it could be inferred that blue-yellow color vision is more impaired during both acute and chronic high IOP, suggesting that small-field bistratified ganglion cells are more susceptible to increased IOP compared to midget ganglion cells, regardless of the type of IOP elevation. This differs from our findings that there is the distinction in the tolerance to acute and chronic IOP elevation between magnocellular (parasol ganglion cells) and parvocellular cells (midget ganglion cells) (Li et al., 2019). Numerous studies have demonstrated that magnocellular cells suffer selective loss compared to parvocellular cells at the early stages of chronic glaucoma in patients and in chronic ocular hypertension animal models (Zhang et al., 2016; Dandona et al., 1991; Quigley et al., 1988; Quigley et al., 1987). Our previous studies that examined the effects of acute IOP elevation on the visual acuity of non-human primates and pioneering electrophysiological studies in the cat show relatively greater dysfunction in parvocellular cells compared to magnocellular cells during acute IOP elevation (Chen et al., 2003; Li et al., 2019). This might be due to metabolic and anatomic differences. For example, magnocellular cells may have more intracellular reserves of ATP, oxygen and potassium than parvocellular cells during short-term acute IOP elevation (Grehn, 1981). However, the present study reveals that the difference of the tolerance to acute IOP elevation between small-field bistratified and midget ganglion cells is quite similar to chronic IOP elevation. We speculate that since small-field bistratified ganglion cells have a unique morphology and connectivity to second order neurons (Kolb et al., 1997; Martin, 1998), this complexity might increase their oxygen consumption, thus reducing the tolerance of small-field bistratified cells to increased IOP, whether acute or chronic. The exact details of the underlying mechanisms need further investigation.

4.3. Impact of acute high IOP on the magnocellular, parvocellular and koniocellular pathways

Our previous study shows that fine visual discrimination within the central visual field is impaired during acute sharp IOP elevation in macaque monkeys, implicating relatively greater dysfunction in the parvocellular pathway than the magnocellular pathway in the primate visual pathway (Li et al., 2019). The present study reveals that acute IOP elevation affects cortical color processing and specifically that the blue-yellow responses seem more sensitive than the red-green responses,

implying selective impairment of the koniocellular pathways compared to the parvocellular pathways. Combining these results, we infer that the susceptibility of RGCs to acute high IOP are as follows: small-field bistratified ganglion cells, midget ganglion cells, and then parasol ganglion cells, thus causing the functional loss of the koniocellular pathway, the parvocellular pathway, and the magnocellular pathway successively when IOP increased acutely. Blue-yellow color vision appears to be the most vulnerable visual function during acute IOP elevation. This might be because the abilities of the different types of RGCs to resist the effects of acute raised IOP are different. In our studies, acute IOP elevation was transient and did not cause RGC death, but might initiate the early phase of RGC dysfunction. Whether the functional differences of these three types of RGCs exist when acute high IOP causes apoptosis and atrophy of RGCs needs further exploration in future studies.

5. Conclusions

In summary, the present study examines the immediate effect of acute high IOP on the color responses across V1, V2, and V4 of macaque monkeys. We demonstrate that the cortical color responses are substantially depressed during the acute phase of IOP elevation along with a similar decrement in response magnitude within V1, V2, and V4. This effect was more severe for blue-yellow responses than for red-green responses, suggesting selective impairment of the koniocellular pathways compared with parvocellular pathways. Our study provides suggestive physiological evidences for ophthalmologists that acute glaucoma patients may have blue-yellow color vision defects first.

CRediT authorship contribution statement

Mengwei Li: Conceptualization, Investigation, Formal analysis, Writing – original draft. **Xiaoxiao Chen:** Conceptualization, Investigation, Formal analysis, Writing – review & editing. **Nini Yuan:** Supervision, Conceptualization, Investigation, Formal analysis, Writing – review & editing. **Yiliang Lu:** Methodology, Formal analysis, Data curation. **Ye Liu:** Methodology, Writing – review & editing. **Hongliang Gong:** Methodology, Formal analysis. **Liling Qian:** Resources. **Ian Max Andolina:** Data curation. **Jihong Wu:** Resources. **Shenghai Zhang:** Resources. **Niall McLoughlin:** Writing – review & editing. **Xinghuai Sun:** Supervision, Project administration, Funding acquisition. **Wei Wang:** Supervision, Project administration, Funding acquisition, Writing – review & editing.

Declaration of Competing Interest

The authors declare that they have no known competing financial interests or personal relationships that could have appeared to influence the work reported in this paper.

Acknowledgments

This research was supported by the National Natural Science Foundation of China (No.82030027 [XHS], No.81790641 [XHS], and No.81900852 [MWL]); the Strategic Priority Research Program of Chinese Academy of Sciences (No.XDB32060203 [WW]); National Key Research and Development Program of China (No.2020YFA0112700 [XHS]); Clinical Research Plan of SHDC (No.SHDC2020CR6029 [XHS]). The funders had no role in study design, data collection and analysis, decision to publish, or preparation of the manuscript.

References

Alvarez, S.L., Pierce, G.E., Vingrys, A.J., Benes, S.C., Weber, P.A., King-Smith, P.E., 1997. Comparison of red-green, blue-yellow and achromatic losses in glaucoma. Vision Res. 37 (16), 2295–2301.

An, X., Gong, H., Qian, L., Wang, X., Pan, Y., Zhang, X., Yang, Y., Wang, W., 2012. Distinct functional organizations for processing different motion signals in V1, V2, and V4 of macaque. J. Neurosci. 32 (39), 13363–13379.

Austin, D.J., 1974. Acquired colour vision defects in patients suffering from chronic simple glaucoma. Trans. Ophthalmol. Soc. U K 94, 880–883.

Bayer, L., Funk, J., Töteberg-Harms, M., 2020. Incidence of dyschromatopsy in glaucoma. Int. Ophthalmol. 40 (3), 597–605.

Chen, X., Sun, C., Huang, L., Shou, T., 2003. Selective loss of orientation column maps in visual cortex during brief elevation of intraocular pressure. Invest. Ophthalmol. Vis. Sci. 44, 435–441.

Conway, B.R., 2014. Color signals through dorsal and ventral visual pathways. Vis. Neurosci. 31 (2), 197–209.

Conway, B.R., Chatterjee, S., Field, G.D., Horwitz, G.D., Johnson, E.N., Koida, K., Mancuso, K., 2010. Advances in color science: from retina to behavior. J. Neurosci. 30 (45), 14955–14963.

Conway, B.R., Moeller, S., Tsao, D.Y., 2007. Specialized color modules in macaque extrastriate cortex. Neuron 56 (3), 560–573.

Dandona, L., Hendrickson, A., Quigley, H.A., 1991. Selective effects of experimental glaucoma on axonal transport by retinal ganglion cells to the dorsal lateral geniculate nucleus. Invest Ophthalmol Vis Sci 32, 1593–1599.

Drance, S.M., Lakowski, R., Schulzer, M., Douglas, G.R., 1981. Acquired color vision changes in glaucoma. Use of 100-hue test and Pickford anomaloscope as predictors of glaucomatous field change. Arch. Ophthalmol. 99, 829–831.

Dussan Molinos, L., Huchzermeyer, C., Lämmer, R., Kremers, J., Horn, F.K., 2022. Blue-yellow VEP with projector-stimulation in glaucoma. Graefes Arch. Clin. Exp. Ophthalmol. 260 (4), 1171–1181.

Ferster, D., 1992. The synaptic inputs to simple cells of the cat visual cortex. Prog. Brain Res. 90, 423–441.

Foster, P.J., Johnson, G.J., 2001. Glaucoma in China: how big is the problem? Br. J. Ophthalmol. 85, 1277–1282.

Gegenfurtner, K.R., 2003. Cortical mechanisms of colour vision. Nat. Rev. Neurosci. 4 (7), 563–572.

Greenstein, V.C., Halevy, D., Zaidi, Q., Koenig, K.L., Ritch, R.H., 1996. Chromatic and luminance systems deficits in glaucoma. Vision Res. 36 (4), 621–629.

Grehn, F., 1981. The sensitivity of the retinal nerve fibre layer to elevated intraocular pressure and graded hypoxia in the cat. Vision Res. 21 (11), 1697–1701.

Gunduz, K., Arden, G.B., Perry, S., Weinstein, G.W., Hitchings, R.A., 1988. Color vision defects in ocular hypertension and glaucoma. Quantification with a computer-driven color television system. Arch. Ophthalmol. 106, 929–935.

Hendry, S.H.C., Reid, R.C., 2000. The koniocellular pathway in primate vision. Annu. Rev. Neurosci. 23 (1), 127–153.

Heron, G., Adams, A.J., Husted, R., 1988. Central visual fields for short wavelength sensitive pathways in glaucoma and ocular hypertension. Invest. Ophthalmol. Vis. Sci. 29, 64–72.

Hubel, D.H., Livingstone, M.S., 1987. Segregation of form, color, and stereopsis in primate area 18. J. Neurosci. 7 (11), 3378–3415.

Jonas, J.B., Aung, T., Bourne, R.R., Bron, A.M., Ritch, R., Panda-Jonas, S., 2017. Glaucoma. Lancet 390 (10108), 2183–2193.

Kalmus, H., Luke, I., Seedburgh, D., 1974. Impairment of colour vision in patients with ocular hypertension and glaucoma. With special reference to the "D and H color-rule". Br. J. Ophthalmol. 58 (11), 922–926.

Kolb, H., Goede, P., Roberts, S., McDermott, R., Gouras, P., 1997. Uniqueness of the S-cone pedicle in the human retina and consequences for color processing. J. Comp. Neurol. 386 (3), 443–460.

Korth, M., Nguyen, N.X., Junemann, A., Martus, P., Jonas, J.B., 1994. VEP test of the blue-sensitive pathway in glaucoma. Invest. Ophthalmol. Vis. Sci. 35, 2599–2610.

Landisman, C.E., Ts'o, D.Y., 2002. Color processing in macaque striate cortex: relationships to ocular dominance, cytochrome oxidase, and orientation. J. Neurophysiol. 87 (6), 3126–3137.

Lee, B.L., Wilson, M.R., 2003. Ocular hypertension treatment study (OHTS) commentary. Curr. Opin. Ophthalmol. 14 (2), 74–77.

Li, M., Yuan, N., Chen, X., Lu, Y., Gong, H., Qian, L., Wu, J., Zhang, S., Shipp, S., Andolina, I.M., Sun, X., Wang, W., 2019. Impact of acute intraocular pressure elevation on the visual acuity of non-human primates. Ebiomedicine 44, 554–562.

Liu, Y.e., Li, M., Zhang, X., Lu, Y., Gong, H., Yin, J., Chen, Z., Qian, L., Yang, Y., Andolina, I.M., Shipp, S., Mcloughlin, N., Tang, S., Wang, W., 2020. Hierarchical representation for chromatic processing across macaque V1, V2, and V4. Neuron 108 (3), 538–550.e5.

Lu, H.D., Roe, A.W., 2008. Functional organization of color domains in V1 and V2 of macaque monkey revealed by optical imaging. Cereb. Cortex 18 (3), 516–533.

Lu, Y., Yin, J., Chen, Z., Gong, H., Liu, Y.e., Qian, L., Li, X., Liu, R., Andolina, I.M., Wang, W., 2018. Revealing detail along the visual hierarchy: neural clustering preserves acuity from V1 to V4. Neuron 98 (2), 417–428.e3.

Mantyjarvi, M., Terasvirta, M., 1992. Observations on color vision testing in ocular hypertension and glaucoma. Int Ophthalmol 16, 417-422.

Martin, P.R., 1998. Colour processing in the primate retina: recent progress. J. Physiol. 513 (Pt 3), 631–638.

Nassi, J.J., Callaway, E.M., 2009. Parallel processing strategies of the primate visual system. Nat. Rev. Neurosci. 10 (5), 360–372.

Nork, T.M., 2000. Acquired color vision loss and a possible mechanism of ganglion cell death in glaucoma. Trans. Am. Ophthalmol. Soc. 98, 331–363.

Nuzzi, R., Bellan, A., Boles-Carenini, B., 1997. Glaucoma, lighting and color vision. An investigation into their interrelationship. Ophthalmologica 211 (1), 25–31.

Pacheco-cutillas, M., Edgar, D.F., Sahraie, A., 1999. Acquired colour vision defects in glaucoma-their detection and clinical significance. Br. J. Ophthalmol. 83 (12), 1396–1402.

Papaconstantinou, D., Georgalas, I., Kalantzis, G., Karmiris, E., Koutsandrea, C., Diagourtas, A., Ladas, I., Georgopoulos, G., 2009. Acquired color vision and visual field defects in patients with ocular hypertension and early glaucoma. Clin Ophthalmol 3, 251–257.
Pearson, P., Swanson, W.H., Fellman, R.L., 2001. Chromatic and achromatic defects in patients with progressing glaucoma. Vision Res. 41 (9), 1215–1227.
Poinoosawmy, D., Nagasubramanian, S., Gloster, J., 1980. Colour vision in patients with chronic simple glaucoma and ocular hypertension. Br. J. Ophthalmol. 64 (11), 852–857.
Polo, V., Larrosa, J.M., Pinilla, I., Perez, S., Gonzalvo, F., Honrubia, F.M., 2002. Predictive value of short-wavelength automated perimetry: a 3-year follow-up study. Ophthalmology 109 (4), 761–765.
Quigley, H.A., Dunkelberger, G.R., Green, W.R., 1988. Chronic human glaucoma causing selectively greater loss of large optic nerve fibers. Ophthalmology 95, 357–363.
Quigley, H.A., Sanchez, R.M., Dunkelberger, G.R., L'Hernault, N.L., Baginski, T.A., 1987. Chronic glaucoma selectively damages large optic nerve fibers. Invest Ophthalmol Vis Sci 28, 913–920.
Racette, L., Sample, P., 2003. Short-wavelength automated perimetry. Ophthalmol Clin North Am 16 (2), 227–236.
Sample, P.A., 2000. Short-wavelength automated perimetry: it's role in the clinic and for understanding ganglion cell function. Prog. Retin. Eye Res 19 (4), 369–383.
Sample, P.A., Boynton, R.M., Weinreb, R.N., 1988. Isolating the color vision loss in primary open-angle glaucoma. Am. J. Ophthalmol. 106 (6), 686–691.
Sample, P.A., Weinreb, R.N., Boynton, R.M., 1986. Acquired dyschromatopsia in glaucoma. Surv. Ophthalmol. 31 (1), 54–64.
Song, P., Wang, J., Bucan, K., Theodoratou, E., Rudan, I., Chan, K.Y., 2017. National and subnational prevalence and burden of glaucoma in China: A systematic analysis. J Glob Health 7, 20705.
Sun, X., Dai, Y., Chen, Y., Yu, D.Y., Cringle, S.J., Chen, J., Kong, X., Wang, X., Jiang, C., 2017. Primary angle closure glaucoma: What we know and what we don't know. Prog Retin Eye Res 57, 26–45.
Tanigawa, H., Lu, H.D., Roe, A.W., 2010. Functional organization for color and orientation in macaque V4. Nat. Neurosci. 13 (12), 1542–1548.
Ts'o, D.Y., Frostig, R.D., Lieke, E.E., Grinvald, A., 1990. Functional organization of primate visual cortex revealed by high resolution optical imaging. Science 249 (4967), 417–420.
Weinreb, R.N., Aung, T., Medeiros, F.A., 2014. The pathophysiology and treatment of glaucoma: a review. JAMA 311, 1901–1911.
Weinreb, R.N., Leung, C.K., Crowston, J.G., Medeiros, F.A., Friedman, D.S., Wiggs, J.L., Martin, K.R., 2016. Primary open-angle glaucoma. Nat. Rev. Dis. Primers 2, 16067.
Yamagami, J., Koseki, N., Araie, M., 1995. Color vision deficit in normal-tension glaucoma eyes. Jpn. J. Ophthalmol. 39, 384–389.
Yuan, N., Li, M., Chen, X., Lu, Y., Fang, Y., Gong, H., Qian, L., Wu, J., Zhang, S., Shipp, S., Andolina, I.M., Sun, X., Wang, W., 2020. Immediate impact of acute elevation of intraocular pressure on cortical visual motion processing. Invest. Ophthalmol. Vis. Sci. 61 (5), 59.
Zhang, P., Wen, W., Sun, X., He, S., 2016. Selective reduction of fMRI responses to transient achromatic stimuli in the magnocellular layers of the LGN and the superficial layer of the SC of early glaucoma patients. Hum Brain Mapp 37, 558–569.